AD_____

Award Number: DAMD17-98-1-8054

TITLE: Dynamic Functional Mammoscopy: A Non-Ionizing Imaging Technique Enhancing Early Detection of Breast Cancer

PRINCIPAL INVESTIGATOR: Suzanne J. Smith, M.D.

CONTRACTING ORGANIZATION: Columbia University in the City of New York
New York, NY 10032

REPORT DATE: April 2003

TYPE OF REPORT: Final

PREPARED FOR: U.S. Army Medical Research and Materiel Command
Fort Detrick, Maryland 21702-5012

# REPORT DOCUMENTATION PAGE

Form Approved
OMB No. 074-0188



| 1. AGENCY USE ONLY (Leave blank) | 2. REPORT DATE | 3. REPORT TYPE AND DATES COVERED |
|---|---|---|
| | April 2003 | Final (1 Oct 1998 - 31 Mar 2003) |

**4. TITLE AND SUBTITLE**

Dynamic Functional Mammoscopy: A Non-Ionizing Imaging Technique Enhancing Early Detection of Breast Cancer

**5. FUNDING NUMBERS**

DAMD17-98-1-8054



**6. AUTHOR(S)**

Suzanne Smith, M.D.

**7. PERFORMING ORGANIZATION NAME(S) AND ADDRESS(ES)**

Columbia University in the City of New York
New York, NY 10032

E-Mail: sjs@columbia.edu

**8. PERFORMING ORGANIZATION REPORT NUMBER**

**9. SPONSORING / MONITORING AGENCY NAME(S) AND ADDRESS(ES)**

U.S. Army Medical Research and Materiel Command
Fort Detrick, Maryland 21702-5012

**10. SPONSORING / MONITORING AGENCY REPORT NUMBER**

**11. SUPPLEMENTARY NOTES**

Original contains color plates: ALL DTIC reproductions will be in black and white

**12a. DISTRIBUTION / AVAILABILITY STATEMENT**

Approved for Public Release; Distribution Unlimited

**12b. DISTRIBUTION CODE**

**13. ABSTRACT (Maximum 200 Words)**

During the third and final year of this study, we focused on improving the imaging technology of Dynamic Functional Optical Mammoscopy (DFOM) and focused on technique on refining existing weaknesses in specificy identified during the second year of study. In addition, we summarize the case studies and analysis of data obtained during the first two years. This data included optical imaging of patients scheduled for biopsy of breast lesions. These patients were recommended for core or excisional breast biopsy on the basis of equivocal mammographic and ancillary clinical findings within ACR BI-RADS™ categories 3 or 4. Analysis of test results of 117 patients showed that DFOM modality detected cancer in 13 of the 15 patients in whom biopsies confirmed malignant lesions, giving a sensitivity of 87%. DFOM also correctly identified 79 of 102 benign lesions giving a specificity of 77%. In clinical practice, the adjunctive use of DFOM would have decreased the percentage of biopsies that turn out to be benign from 102/117 (87%) to 23/117 (20%). The negative predictive value, the chance that a negative DFOM result truly indicates a benign lesion, was 79/81 (98%) for the cases included thus far. While encouraging, these results suggest the need for further patient studies on specificity.

| 14. SUBJECT TERMS | 15. NUMBER OF PAGES |
|---|---|
| Early Detection, Optical Imaging, Breast Cancer, Blood Profusion | 22 |
| | 16. PRICE CODE |

| 17. SECURITY CLASSIFICATION OF REPORT | 18. SECURITY CLASSIFICATION OF THIS PAGE | 19. SECURITY CLASSIFICATION OF ABSTRACT | 20. LIMITATION OF ABSTRACT |
|---|---|---|---|
| Unclassified | Unclassified | Unclassified | Unlimited |

## Table of Contents

# INTRODUCTION

The imaging technology of Dynamic Functional Optical Mammoscopy (DFOM) is a breast scan based upon transmission/absorption of infrared light, which measures the dynamic patterns of breast reactivity of physiological states in response to soft pressures. The DFOM modality focuses on a *functional* rather than a morphological image, expressed by the dynamic patterns of tissue reactivity after mild compression is charted. Pilot study results suggested that this innovative DFOM imaging technique has the potential to determine which mammographically and clinically indeterminate lesions are benign vs. carcinoma and distinguish those lesions that could avoid biopsy. The purpose of the study reported here is to extend the preliminary results of these pilot studies at Columbia Presbyterian Medical Center, using DFOM between mammography and biopsy to further evaluate the efficacy of DFOM in evaluation of breast lesions, using biopsy results to confirm diagnosis. Our report for the year ending September 30, 2000 summarized results on 47 patients. The total number of patients scanned between June 1, 2000 and September 30, 2001 was 117. Thus a total of 164 patients were included in the study. We point out that many more were scanned but were not included in the study due to the acceptance protocol of the study. This final year report focuses on the tasks targeted in the modifications of Task 3, which focused on the analysis of the dynamic data gathered thus acquired. We addressed in particular, better characterization of blood profusion patterns that characterize lesions, reduction of motion artifacts, with the goal of improve specificity of this optical dynamic imaging technique.

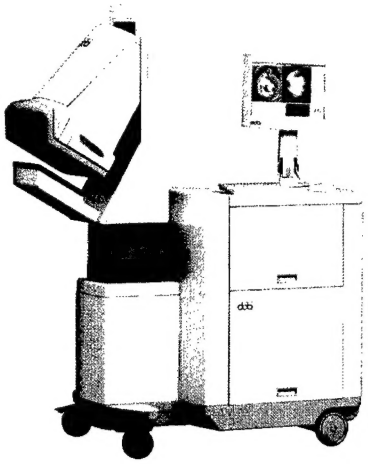

**Figure 1.** Production version of the Dobi Dynamic Optical Breast Imaging system.

# BODY

A total of 189 patients scheduled for biopsy were scanned with the identical protocol between October 1, 2000 and September 30, 2001. The study was performed on women scheduled for core or excisional breast biopsy on the basis of equivocal mammographic and ancillary clinical findings within ACR BI-RADS™ categories 3 or 4. Women who met the selection criteria were enrolled from the normal caseload from both screening and diagnostic mammography. Each woman signed an informed consent prior to being scanned.

The scan procedure required approximately 5 minutes. During examination, the breast was placed in the soft breast holder of the system. The breast was then softly compressed by a thin transparent silicone rubber membrane using an applied pressure of approximately 10 mm Hg. For each scan, the breast was symmetrically centered on the illuminator. When the breast was correctly positioned, illumination adjustment and image recording took place following the requirements of the pressure profile.

Optical illumination was provided by an array of red light emitting diodes (LEDs) attached to the bottom surface of the soft breast holder. Light transmitted through the breast was recorded as a temporal sequence for approximately 30 - 45 seconds by a highly sensitive digital CCD camera. The image sequences were accumulated in digital memory and processed by proprietary software to accentuate differences in the temporal variations of intensity between normal/benign and malignant tissue.

Each woman was scanned by a trained technologist prior to biopsy. The scans were read by an experienced reader trained in interpreting the scans. Results were reported as either a recommendation for biopsy or a recommendation that the woman be sent to interval follow-up.

Recommendations on the basis of DOFM were compared to pathology reports of malignant or benign which were used as the gold standard. Sensitivity, specificity, and negative predictive value were calculated.

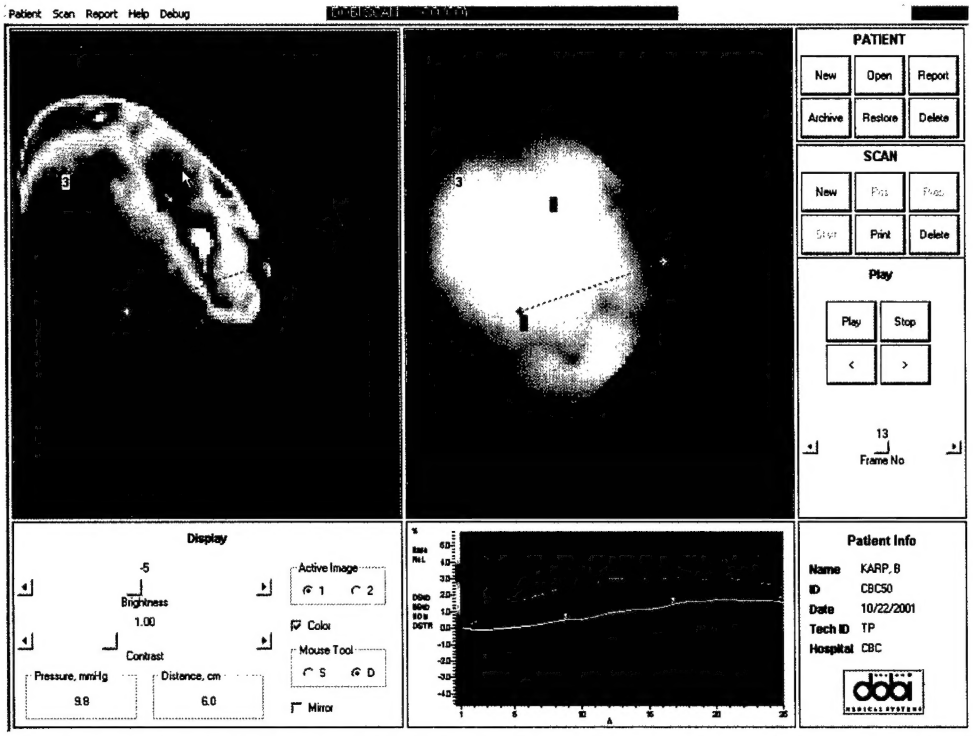


**Figure 2.** Sample abnormal or suspicious case. Note the different profusion rate observed in region 1, as shown in the dynamic curve (red).

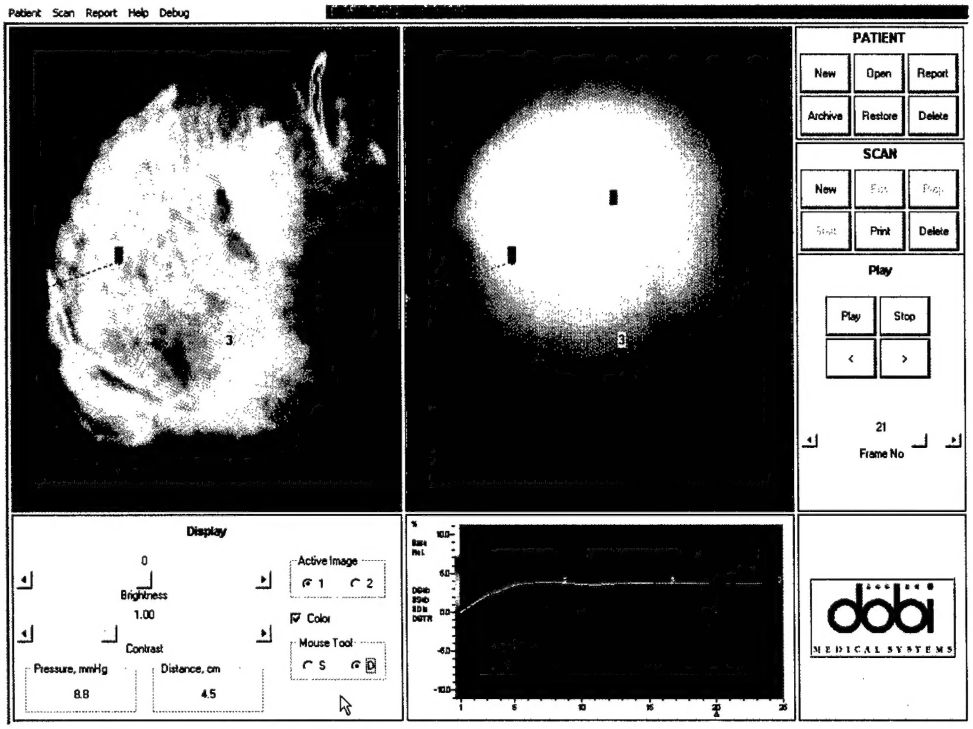


**Figure 3.** Sample results for a normal scan. Note the similarity of curves tracking dynamic profusion rates over areas 1, 2 and 3 in the breast.

Table 1 gives the patient accounting for the 189 patients reported.

**TABLE 1 – Patients Scanned October 1 – September 30, 2001**

| | |
|---|---|
| Excluded patients* | = 36 |
| Unacceptable scans** | = 36 |
| Interpreted scans | = 117 |
| Total scans performed | = 189 |

*Patients who did not meet the selection criteria for the development study protocol.
**Patients whose scans were not acceptable to be interpreted.

Table 2 presents the reasons for scans determined to be unacceptable.

**TABLE 2 – Unacceptable Scans**

| | |
|---|---|
| Lesion sub areolar or located where it cannot be properly illuminated | = 1 |
| Inadequate illumination in area of pathology | = 1 |
| Device related | = 0 |
| Incorrect illumination | = 1 |
| Not enough breast tissue in holder | = 0 |
| Excessive patient movement | = 5 |
| No case report form | =28 |
| Total | =36 |

Table 3 presents patient demographics of race and age.

**TABLE 3 – Patient Demographics**

| | |
|---|---|
| Race | |
| White | = 69 |
| African American | = 15 |
| Hispanic White | = 55 |
| Hispanic Black | = 16 |
| Hispanic | = 2 |
| Asian | = 1 |
| Other | = 3 |
| No data | = 28 |
| Total | = 189 |

AGE: Average = 53
Range = 20-91

Table 4 presents the reasons for excluded scans.

**TABLE 4 – Excluded Scans**

| | |
|---|---|
| Lesion sub areolar or located where it cannot be properly illuminated | = 14 |
| Previous surgery in the ipsiateral breast | = 1 |
| BI-RADs 5 lesion | = 2 |
| Post-menopausal with a palpable lesion | = 1 |
| Not all records available | = 13 |
| Age >74 | = 3 |
| Small breast that cannot be properly illuminated | = 1 |
| Patient unable to remain still | = 1 |
| Total | = 36 |

Table 5 presents the results of scan interpretation.

TABLE 5– Results of 117 Patients Scheduled for Biopsy

| | | *Pathology* | | |
|---|---|---|---|---|
| | | Malignant | Benign | Total |
| **DFOM Recommendation** | Biopsy | 13 | 23 | 36 |
| | Interval Follow-Up | 2 | 79 | 81 |
| | Total | 15 | 102 | 117 |

Sensitivity: 13/15 (87%)
Specificity: 79/102 (77%)
Negative Predictive Value (NPV): 79/81 (98%)

The analysis of test results on the 117 patients with interpreted scans shows that the DFOM detected cancer in 13 of the 15 patients in whom biopsies confirmed malignant lesions ("true positives"). This results in a sensitivity of 87%. The system also correctly identified 79 of 102 benign lesions ("true negatives"). In other words, the specificity of the DFOM was 79/102 (77%).

## Modification of Task 3

During the second year, our discussions with personnel at DOBI Medical Systems suggested that better analysis of the current data before proceeding with an evaluation of screening high risk women would be desirable. Specifically, due to subtle problems in the acquisition of dynamic data we recognized that sensitivity and specificity were not where they could be. Thus during the final year of this project, we proposed to focus on improving the quality of the data in the following areas:

1) *Artifact Removal* - This task involves non-linear filtering to remove imaging artifacts caused by near surface structures such as vessels, tattoos and skin pigmentation. These objects create contrast in our images that are undesirable. Our goal is to apply a filter algorithm that would remove these artifacts while preserving contrast created by deep lesions.

2) *Motion Detection* - Patient motion has been an ongoing problem with DOBI Medical's imaging modality. Motion can be generated by a number of ways, such as normal respiratory movement, heartbeats, the patient moving due to stress. We can estimate this motion by looking at edge effects. We will apply a motion detection algorithm to estimate the amount of movement during acquisition.

3) *Simplified Tumor Model* - DOBI Medical has developed a rather complex model for the hemodynamics in a tumor. The model has not been validated and could take a significant effort to quantify the parameters associated with this model. We would like to jointly work with the technical staff at DOBI on a simplified model that could be verified.

4) *Complex Data Presentation* - DOBI Medical needs better ways to present complex data to the physician. Currently we produce a static image of intensity and a cine loop of dynamic intensity over time. In the future we will be presenting such parameters as a map of change in absorption, a map of intensity, a map of direction vectors associated with increasing or decreasing absorption. We would like to jointly work with DOBI on presenting these complex data sets to physicians in a more intuitive presentation format.

In the next section we describe accomplishments with respect to these goals. This work reflects significant contributions from the Dobi research team, specifically Ivan Masyukov and Michael Klibanov for their work on developing the phantom and carrying out the experiments on an experimental optical breast imaging platform. In addition, Vladimir Zlatov, John Gardner and Alan Rego of Dobi provided many very useful discussions and help in the breast phantom experiments and volunteer scans.

Below we describe progress achieved since September 2001 on the issue of improvement of DOBI images of malignant and benign breasts. The two key new elements of this work are the substantial use of mathematical modeling of light propagation in breast tissues and use of a single LED light source at a time, as opposed to the former use of many sources simultaneously. We first outline unsolved problems of the standard DOBI scanning technique. Next, we present our new method with the use of a single LED source at a time with total of two sources. We demonstrate that this new technique provides a significant improvement of images for the case of mathematical models, using experimental data obtained from dynamic breast phantoms, as well as for breast tissues without lesions. The main achievement is that we have removed artifacts linked to non-uniform deformation of the breast surface induced by random motion of the breast and breast soft holder compression. Although this result certainly indicates a potential for an essential improvement of images of breasts with lesions, our current results should be viewed only as a promising starting point in the solution of the difficult problem of reliable screening and/or diagnostics by the DOBI device.

**Overview of The Standard DOBI Technique**

In September 2001, we first tried to improve standard DOBI images by applying mathematical models of light propagation in tissues. Soon however we discovered that those models were not applicable to the standard broad illumination data acquisition technique. The main reason was that a mathematical model is usually adapted to the case of a single light source at a time. The standard DOBI procedure uses many sources simultaneously. As a result, light information "mixes up" due to the diffuse nature of light propagation in breast tissues. Another important factor, which negatively affects

standard DOBI images, is due to the random motions of the breast surface. Thus, the effects of those motions are again "mixing up" with the effects produced by changes in the attenuation coefficient $\alpha$, making separation of motion and $\alpha$ impossible. While only the $\alpha$ coefficient, which is directly related to blood volume, oxygenation, and water content levels, is carrying the physiological information necessary for the diagnostics, geometrical shifts of the breast surface do not carry any information useful neither for the diagnostics, nor for the screening purpose.

Therefore, one of our main goals was to remove artifacts linked to those shifts. We are happy to report that this goal was achieved for the case of mathematical models, experimental data obtained from phantoms, as well as for the breast tissues without lesions.

Let $I(x,t)$ be the measured intensity of light at the point $x$ of the breast surface and at the time $t$, and $I_0$ be the initial intensity of light falling on the opposite side of the breast and originated by light sources. Because many light sources are acting simultaneously, one can approximate $I_0$ as a homogeneous plane wave. Further, because this is CW (i.e., constant wave) light, then the governing diffusion equation is

$$\nabla^2 I - \alpha^2 \bullet I = 0 \quad (1.1)$$

Where $\nabla^2$ is Laplace operator, $\alpha = \sqrt{3\mu'_s \bullet \mu_a}$ is the attenuation coefficient, $\mu'_s$ is the reduced scattering coefficient, and $\mu_a$ is the absorption coefficient. Of course, these coefficients are changing inside the breast. However, since there is no tool to recover those internal changes, only integral absorption and scattering coefficients will be considered below, i.e., such an integral coefficient represents a sort of an average along certain volumes inside the breasts.

It was observed experimentally in [1,2] that the reduced scattering coefficient does not change significantly from one point of the breast to another. Only changes of the absorption coefficient are significant. Hence, it will be assumed below that $\mu'_s$ is not changing in time. Thus, our concerns will be only about changes of the attenuation coefficient $\alpha$, assuming that this coefficient actually determines the absorption coefficient $\mu_a$. It is well known that the absorption coefficient is directly linked with such important physiological parameters as blood volume, oxygenation and water content. This stresses the potential importance of estimating of $\mu_a$ both for screening and diagnostic purposes.

Under the above assumptions the following approximate formula can be derived for the light intensity at the point $x$ of the breast surface

$$I(x,t) = I_0 \bullet \exp[-\alpha(x,t) \bullet L(x,t)] \quad (1.2),$$

where $L(x,t)$ is the breast thickness at the point $x$ of the breast surface and at the time $t$. Actually, $L(x,t)$ can be interpreted twofold:

1. The distance between the point $x$ of the breast surface and the closest LED source, in the case of multiple sources applied simultaneously (i.e., in the case of the standard DOBI images).
2. The distance between the point $x$ of the breast surface and the LED source, in the case of a single source at a time.

Remark. Below we will omit sometimes $x$ and $t$ in notations for $L$ and $\alpha$ for brevity.

Let $t = 0$ be the moment of the Pressure Jump and $t_0 > 0$ be a moment of time after the Pressure Jump. Current images of DOBI display function $\varphi_{t_0}(t)$,

$$\varphi_{t_0}(t) = [I(t) - I(t_0)]/I(t_0) = I(t)/I(t_0) - 1 = \Delta I / I$$

Introduce the following notations

$$\Delta\alpha = \alpha(t) - \alpha(t_0), \ \Delta L = L(t) - L(t_0).$$

Hence,

$$\alpha(t) = \alpha(t_0) + \Delta\alpha \text{ and } L(t) = L(t_0) + \Delta L$$

This in combination with (1.2) leads to the following expression for the function $\varphi_{t_0}(t)$

$$\varphi_{t_0}(t) = \Delta I / I = \exp\{-(\Delta\alpha \bullet L(t_0) + \alpha(t_0) \bullet \Delta L + \Delta\alpha \bullet \Delta L)\} - 1$$

Thus, ignoring the small term of the second order $\Delta\alpha \bullet \Delta L \approx 0$ and using the well known formula $\exp(y) - 1 \approx y$, for small values of $y$, we obtain

$$\Delta I / I \approx \Delta\alpha \bullet L + \Delta L \bullet \alpha \quad (1.3)$$

The formula (1.3) represents the standard DOBI image. It is clear from this formula that changes in the attenuation coefficient are mixed with the changes in the breast's thickness due to random movements. This is the major cause of artifacts in those images. Therefore, a new approach to remove those artifacts is described below. By this new procedure we separate changes in the attenuation coefficient from changes in breast thickness.

It is well known that the above mathematical model of light propagation in the breast tissue works the best when breast is illuminated by a single LED source at a time. So, the idea was to acquire images, illuminating the breast by several LED sources

sequentially,using a single source at a time. We needed at least two (2) sources, since we actually have two unknowns at each point of the breast surface and at each moment of time: $\alpha$ and $L$. *The details of this new method are not described in this report to protect the commercial interests of Dobi.* However, we do describe the experimental design and outcomes for both the numerical phantom and the dynamic phantom used in the study.

**Numerical Phantoms**

Numerical experimentation is a convenient way to analyze newly developed algorithms. Experimentation with synthetically generated data has the following obvious advantages:

a. All parameters of the model, such as absorption coefficient, breast profile, LED output power, deformation, etc., are assigned at the beginning, and therefore are known. The latter allows one to compare reconstructed parameter values to the "true" (i.e., assigned) ones. This is not always possible in "field" experiments, because some parameters are unknown, or can be just approximately estimated. A good example of such a parameter is an abnormal vascular volume which is not available from morphological modalities like x-ray mammography. Another example is a breast profile, which can not be measured accurately unless sophisticated and costly equipment is used.
b. Synthetically generated data allows one to vary parameters in a broad range, which either is not achievable in reality or requires quite an effort to accumulate necessary data or costly modification of hardware. For example the influence of the CCD camera parameters on the outcome of the algorithms can be easily found without complex actual experimentation.
c. Once reliable numerical phantom model is developed, optimization of algorithms becomes both less costly and less time consuming process.

However, the mumerical model has only one potential disadvantage, which should be carefully monitored. Equations used to simulate light propagation should describe accurately enough the light propagation process taking place in breast phantoms and real breast. We will indicate later in this report that applied methods yield similar results both on simulated, breast phantoms and real breasts.

In this report, we present the results of a successful comparison for a numerically simulated phantom and the dynamic breast phantom over a variety of illumination conditions, tumor locations, and deformation parameters.

The algorithm of generating synthetic data includes the following main steps:

1. Definition of LED configuration. Standard DOBI illuminator was integrated into the numerical model. It includes 127 LEDs placed on a grid with 1cm step. Each LED has a diameter of 5 mm, and a variable output power. Any number of LEDs can be turned on at any time. For numerical simulations presented in this report we used sequential scanning of 9 LEDs in a horizontal row with the 1cm step.

2. Definition of breast surface profile. The developed numerical model allows one to assign any breast shape. For brevity, we used partially elliptical shape of the breast, with the maximum thickness of 6 cm.
3. Definition of image format and CCD camera field of view. Standard DOBI image format of 102x128 was used.
4. Definition of normal tissue optical properties. Absorption coefficient was assigned to 0.05 1/cm, and scattering coefficient was 10 1/cm. Normal tissue was considered uniform and the parameters did not change with time.
5. Definition of tumor parameters. The tumor was located above the $7^{th}$ LED at 3 cm depth and had a diameter of 1 cm. Scattering coefficient did not depend on time and was equal to 10 1/cm. The absorption coefficient changed from 0.05 1/cm to 0.1 1/cm.
6. Images were generated using the small perturbation approach for the tumor model. In other words, the tumor presence acts as a secondary light source at the tumor location. The amplitude of this light source is proportional to tumor volume, absolute change of absorption coefficient and photon density created by illuminator at the tumor location. A formula was used to calculate the light propagation from LEDs and tumor location to the surface of the breast.
7. The sequence of images generated consisted of 27 images. The first 9 images were generated for 9 sequential LEDs using original breast profile, and no tumor was added. Non-uniform deformation of the breast was added to the following 9 images. The thickness deformation profile varied from 0.6 mm on the left side of the breast to -0.6 mm on the right side, i.e. the breast was simulated to become thicker on the left side, and thinner on the right. This represented a typical motion of the breast observed on clinical data (the patient moved to the left). A tumor was added to the last 9 images. Depending on the frames loaded during data processing step, the generated sequence allowed to analyze different LED locations with respect to tumor, motion artifact alone, tumor image alone as well as tumor image with motion artifact present.
8. CCD filter was applied to the sequence of images, adding readout and shot noise, bias level, and conversion to 14-bit format. Typical Apogee AP-260 CCD camera parameters were used.
9. The images were converted and saved in standard DOBI data file format. Proper dark frame was added.

The following are the processing steps performed for all images presented in this section of the report:

1. Load proper image subsequence. For example, if images created by LEDs number 6 and 8 for just surface deformation in numerical phantom experiments are in question, the subsequence should be 6, 8, 15, and 17.
2. Select an area of interest. A rectangular area of 61 pixels wide and 41 pixels high was used.
3. Calculate standard DOBI image, Alpha image, and Q image according to algorithms described in the previous sections of this report.
4. Display 3 images in color and gray scale.

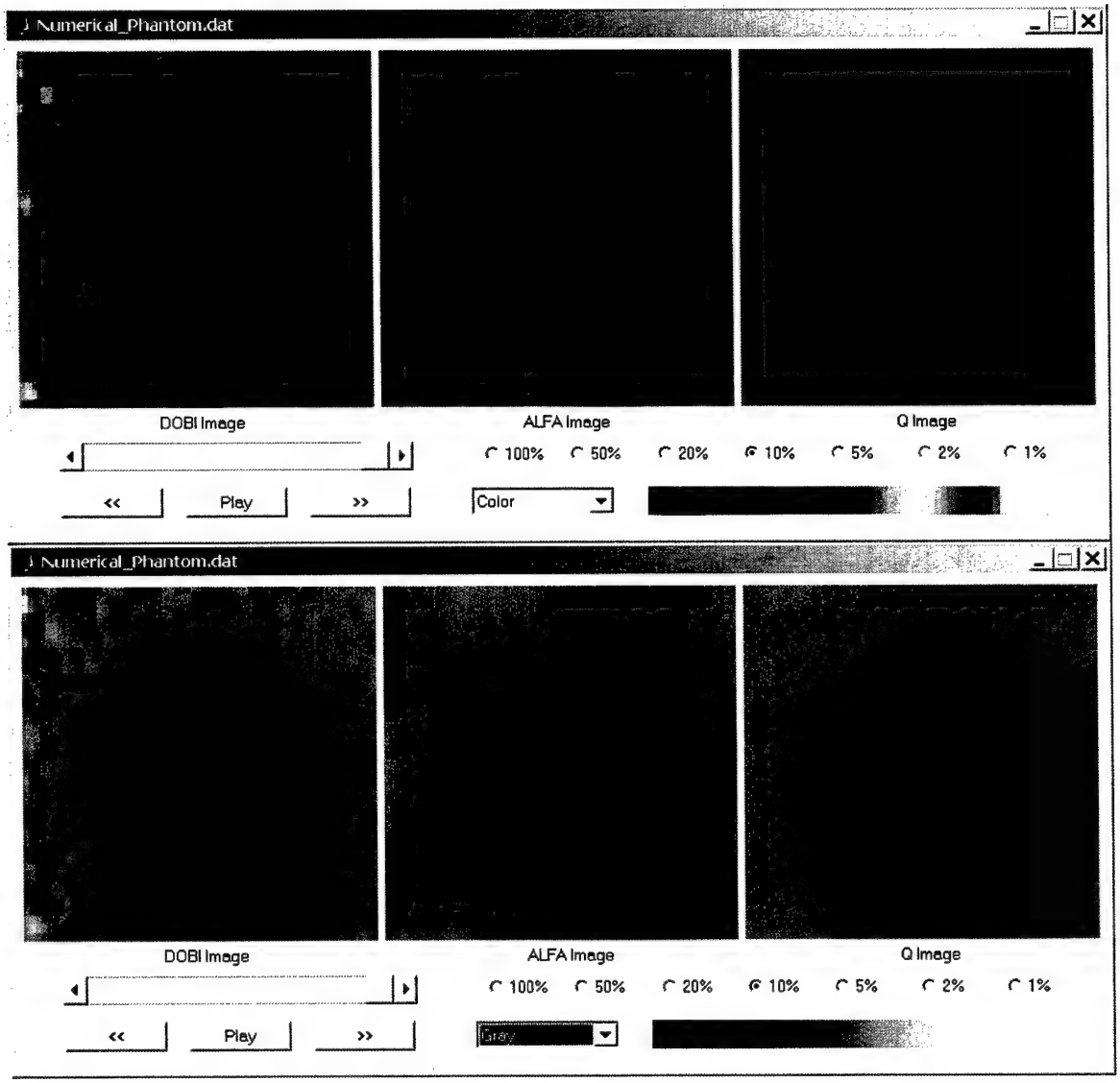


**Figure 4.** Numerically Simulated Phantom. The lesion is located between LEDs. No motion added. Images pairs loaded [(15 17) (24 26)].

All three images demonstrate similar contrast. Alpha and Q images have less noise because of the excellent noise removal techniques of the spline methods used. This example demonstrates that if no motion artifact is present, all three methods can reveal the presence of the tumor.

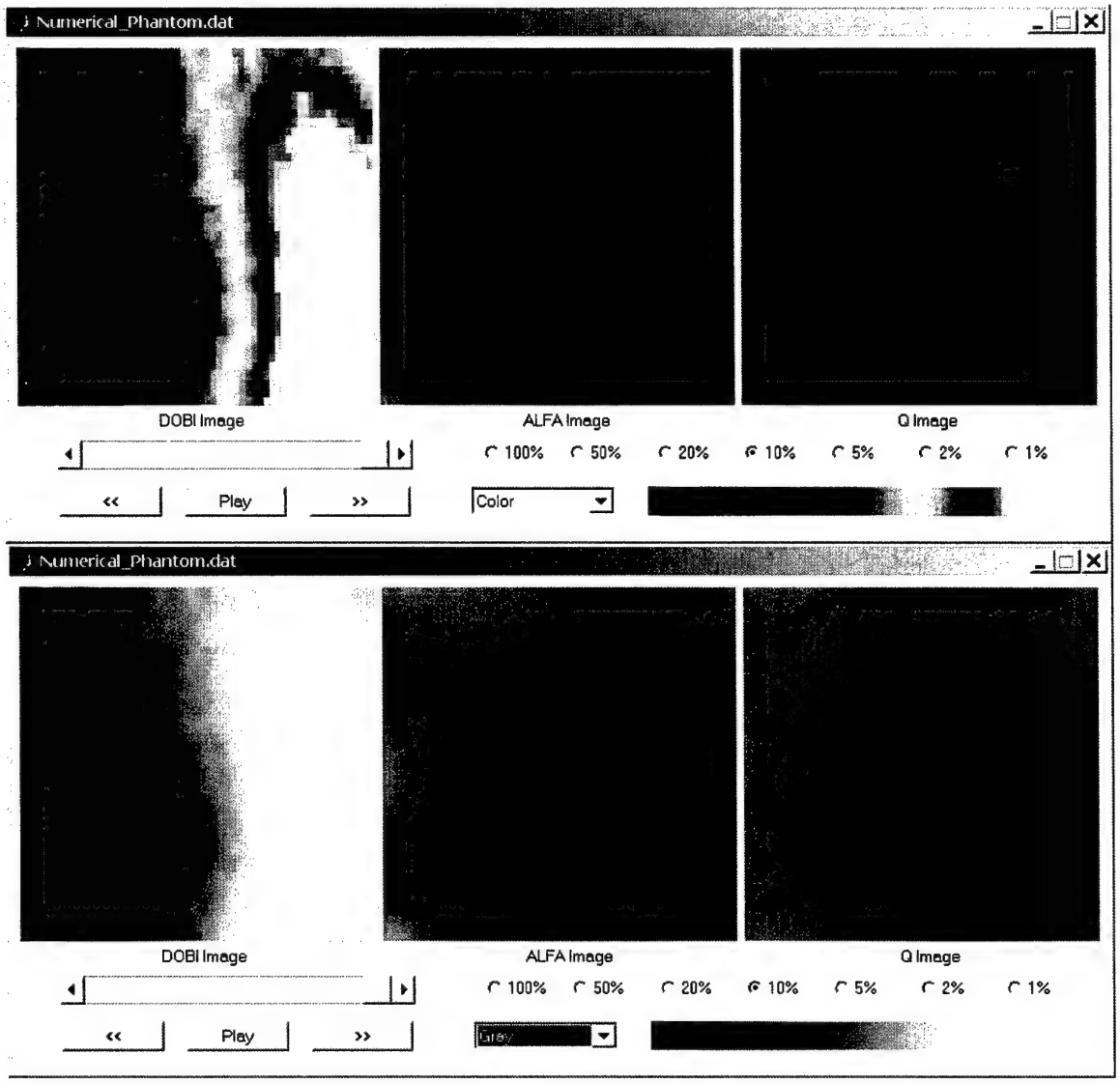


**Figure 5.** Numerically Simulated Phantom. The lesion is located between LEDs. Motion added. Images pairs loaded [(6 8) (24 26)].

DOBI image contrast created by the lesion is totally masked by the motion artifact. Alpha and Q images reveal the lesion presence, and are not sensitive to motion deformation. The contrast on Alpha and Q images is similar to the contrast on Figure 4, where no motion was added

**Dynamic Breast Phantom**

We used a specially developed dynamic phantom that has mechanical and optical properties similar to those of the human breast.

The phantom was made from mix of water, gelatin, and milk powder. A proper concentration of the milk powder was found to simulate the absorption and scattering properties of the breast. The phantom was built 6 cm thick, and 13 cm in diameter.

The lesion was simulated by 3-4 turn nut made from transparent plastic tube. Two such "lesions" were inserted in the phantom. The lesions were 2 and 4cm in diameter. The lesions were located close to the center of the phantom about 2 cm apart.

Food die was used to simulate the dynamic lesion behavior. The concentration of the die was adjusted to obtain typical 5% contrast on standard DOBI images. The dynamic absorption change was performed by means of the valve module controlling the die and pure water flow through the lesions.

The following steps were performed to construct the phantom:

1) 750 ml Hot Water (From a coffee unit close to boiling)
2) Four 3.2 oz. Packs of Instant Nonfat Dry Milk (ShopRite brand)
3) 2.2 oz. Infant Formula powder (Nestle Carnation Good Start)
4) Six 7gram packages of Unflavored Gelatin (Knox original Gelatin)
5) Mix ingredients using the pulse mode of the blender. Pulse the blender approximately once every two seconds. Mix for about 1/2 minutes. This helped reduce foaming.
6) Coat the container you will cure the phantom in with petroleum jelly.
7) Fix simulated tumors in desired location using a set-up jig.
8) Pour liquid into container but try to minimize the surface foam in the mixer container.
9) Refrigerate the phantom for at least 4 hours.
10) Wrap phantom in cellophane.
11) Test phantom for optical properties.

The LED scanning protocol consisted of 27 LEDs formed by 3 rows of LEDs. We used the $3^{rd}$ , $5^{th}$, and $7^{th}$ rows of the DOBI illuminator. Each row contained 9 LEDs with 1cm of separation.

Soft holder pressure and tumor absorption dynamics were made periodic with a 90° phase shift, allowing us to analyze different combinations tumor dynamics, illumination location, surface deformation due to change in the soft holder pressure, and depth of the lesion.

For comparison purposes, all images shown in the figures below are presented using standard DOBI algorithm, and Alpha and Q methods.

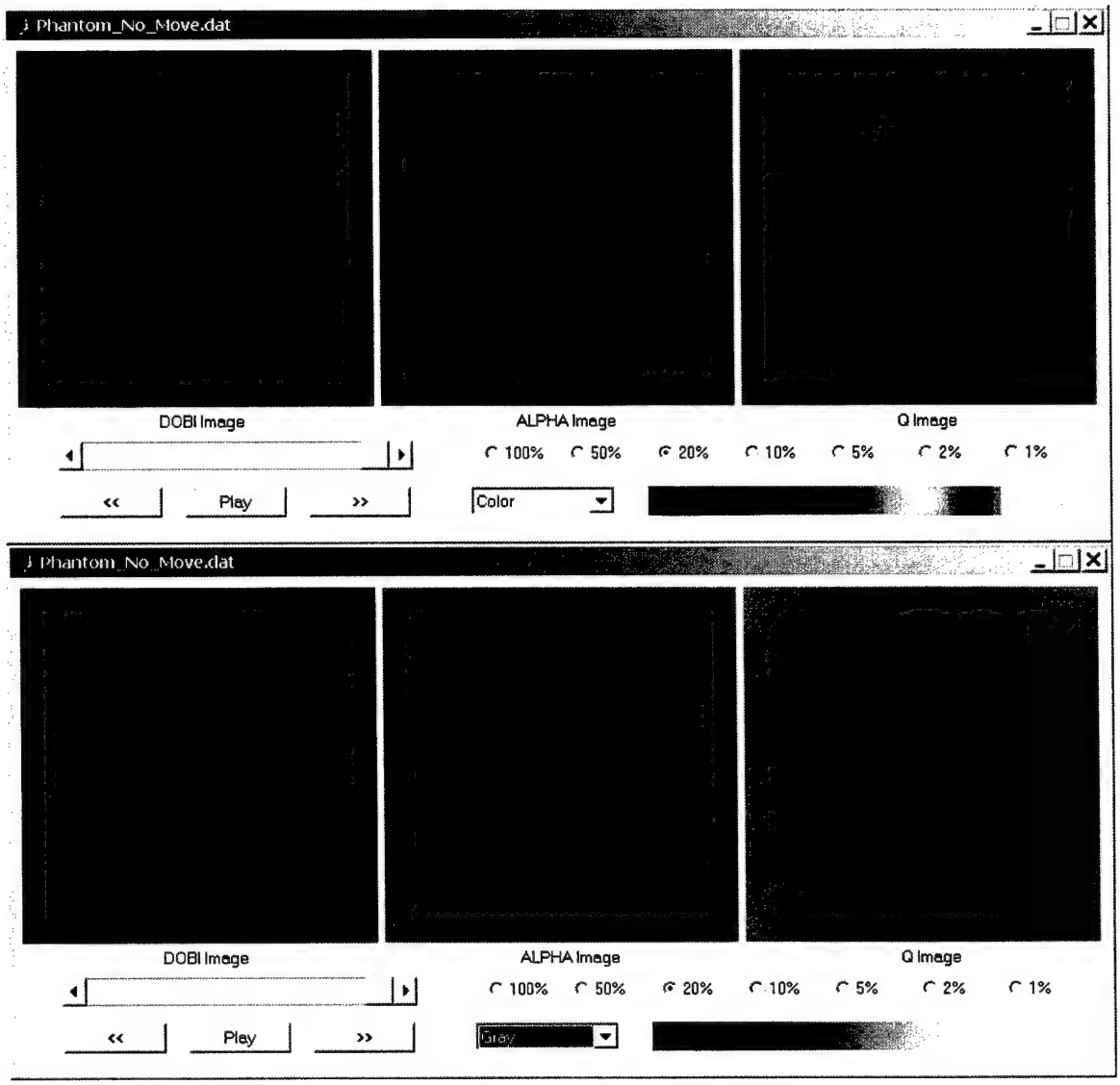


**Figure 6.** Breast Phantom. The lesion is 4 cm deep. No motion.
Images pairs loaded [(4 6) (544 546)].

The lesion was located at 2cm and 4cm deep (only shown). At the 4cm depth, the lesion can be hardly detected on the DOBI image due to heavy broadening of the contrast profile. The broadening is also visible on the Alpha image. Q-image demonstrates the narrowest contrast profile.

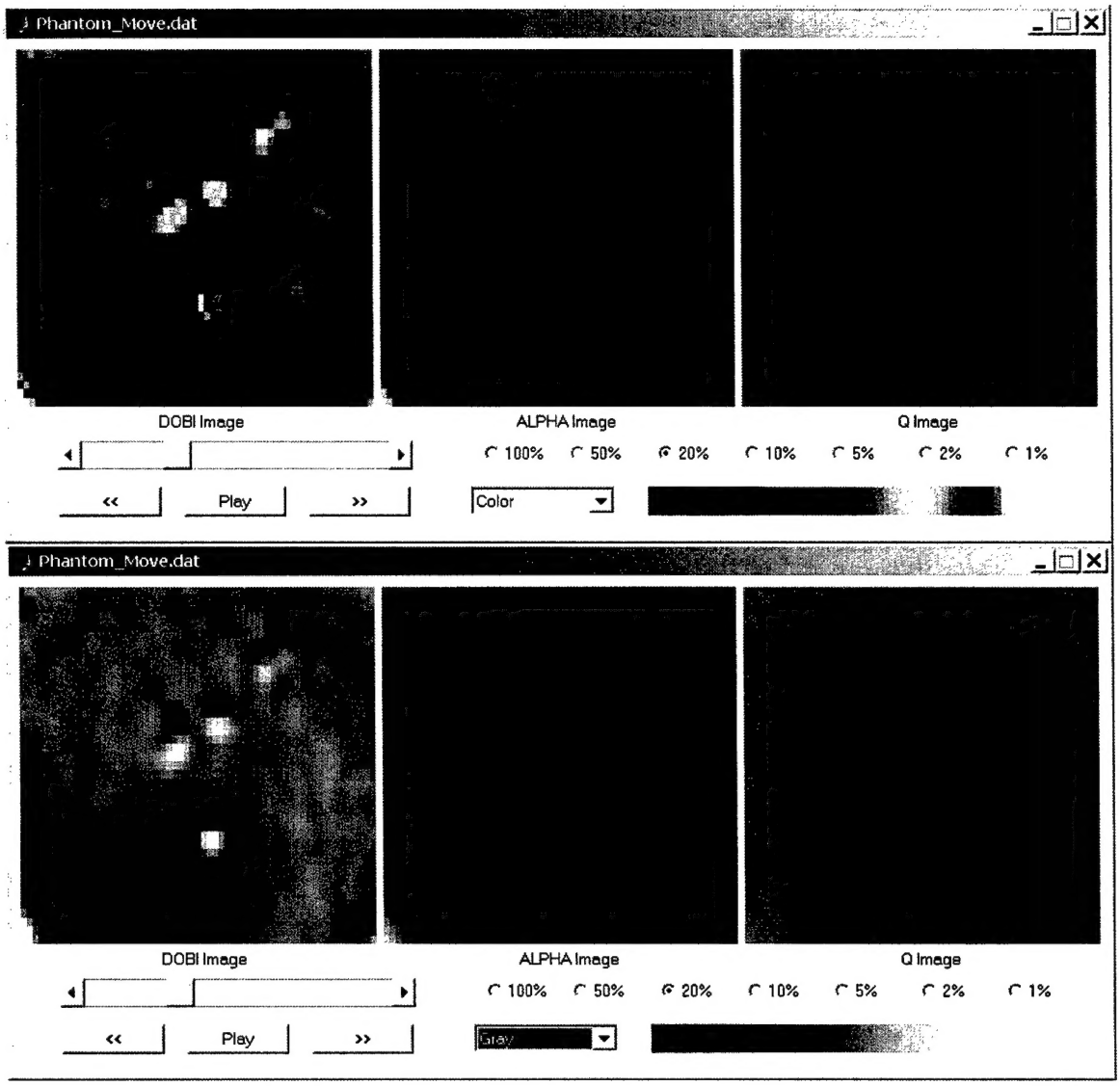


**Figure 7.** Breast Phantom. The lesion is 4 cm deep. Motion.
Images pairs loaded [(4 6) (274 776)].

Note that the lesion contrast on the DOBI image is completely masked by motion artifact. Detailed analysis showed that broadened dark contrast created by the lesion was compensated by thinning of the phantom due to pressure jump. Alfa and Q images are not sensitive to motion. Q-image demonstrates the least broadening of the contrast even for rather deep lesion (4 cm deep).

## Normal Volunteer Scan Example

To evaluate new algorithms we used scan data obtained on healthy volunteers using a scanning protocol of 6 LEDs. The two center LEDs on the 1st row of the DOBI LED illuminator were used. These LED were located 2 cm apart.

Figure 8 show images corresponding to a pressure jump and the contrast developed on the 10 mmHg plateau.

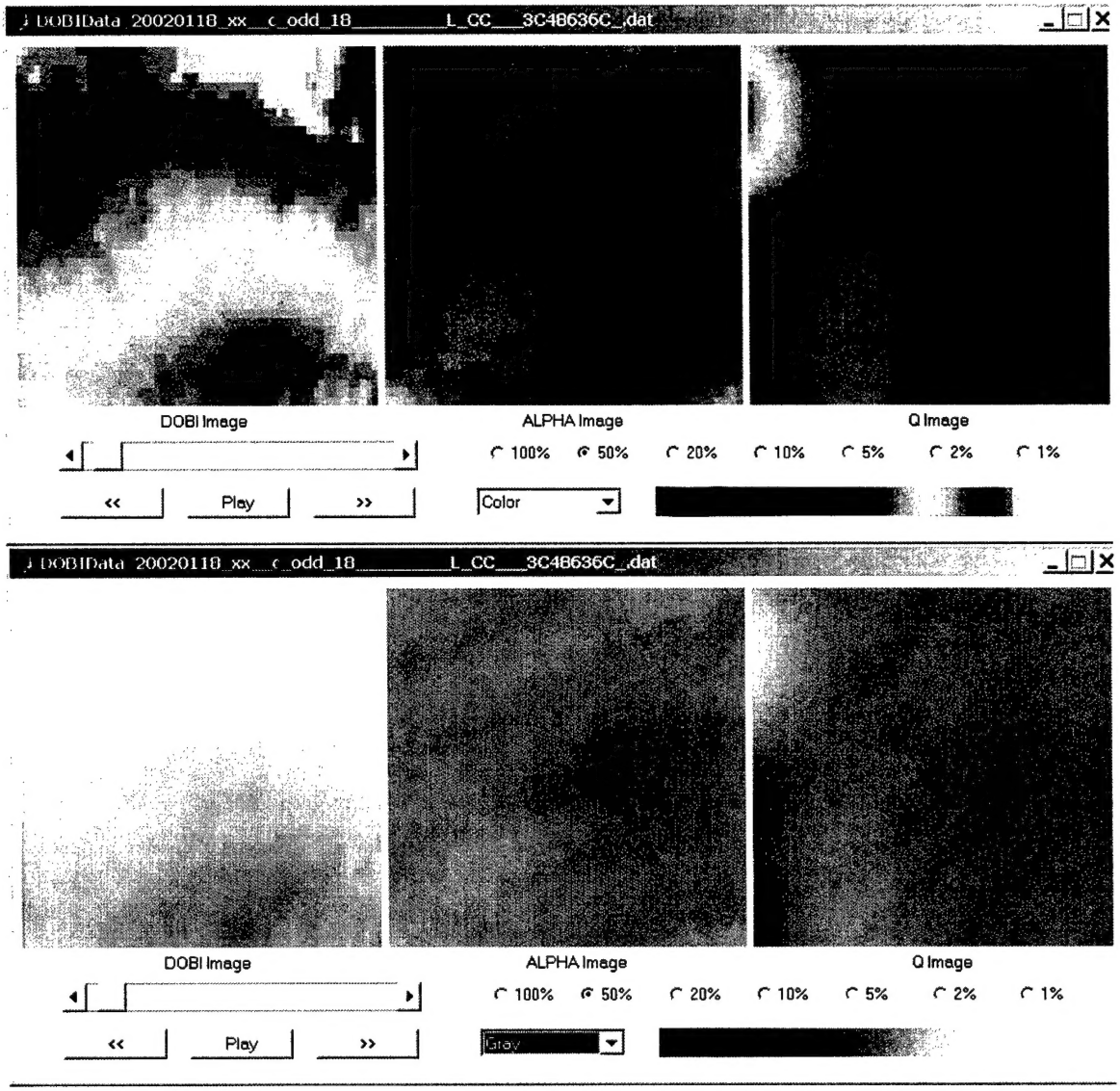


**Figure 8.** Normal Volunteer. Contrast generated by pressure jump.
Images pairs loaded [(79 81) (91 93)].

In Figure 8 above, the DOBI image demonstrates a deformation contrast similar to a typical "chest wall" artifact contrast. This may be caused by increased deformation of the breast in the areas near the nipple (top portion of the image). Alfa and Q images show a reduced sensitivity to non-linear motion induced by a pressure jump. Note, that the motion artifact removal is very similar to the synthetically simulated data shown earlier. This results validates the accuracy of our mathematical model.

# KEY RESEARCH ACCOMPLISHMENTS

1. We confirmed that indeed DOBI Images are very sensitive to motion artifacts.
2. The crucial conclusion of the above effort is that surface motion, which was the main unsolved problem of standard DOBI images DOBI, are ELIMINATED almost completely by new algorithms (although, so far only for phantom media and mathematically simulated data ). In our opinion, the ratio between signal and motion artifact is increased by at least a factor of five.
3. The $\alpha$ image provided good results when the pathology was "between" LED sources. The $Q$ image, however provides good results for both scenarios: when pathology was between and off sources. On the other hand, the $\alpha$ image gives one a value of the attenuation coefficient $\alpha$. This seems to be important for diagnostics. The $Q$ image, however does not provide the value of $\alpha$.
4. We suggest that both images should be used. One can imagine a scenario when sources are placed off the pathology. In this case $Q$ image would tell one, where the sources should be placed. After such a new placement is done, the $\alpha$ image would provide the value of $\alpha$ in the pathology area.
5. Comparison of images of normal volunteers with the images of a numerical phantom shows strong similarities which give confidence to the adequacy of the mathematical model and applied algorithms.
6. We have successfully completed the main goals of the this phase of the project (Task 3) in investigating problems related to (a) Artifact removal, (b) Motion detection, (c) Tumor profusion models, and (d) Presentation of temporal data.

# REPORTABLE OUTCOMES

We expect to publish these results in collaboration with the research team at Dobi. However given the commercial interests of Dobi, the publication will require clearance and approval prior to submission.

# CONCLUSIONS

Given the improvement in the new algorithms described in this report, we believe that improved specificity of the Dobi imaging protocol will improve. The indications of effectiveness of this new modality are very encouraging. To the extent of the cases studied prior to this improvement, the results previously reported indicate that the adjunctive use of the DOFM in clinical practice would have decreased the percentage of biopsies that turn out to be benign from 102/117 (87%) to 23/117 (20%). The negative predictive value, the chance that a negative DFOM result truly indicates a benign lesion, is 79/81 (98%).

# REFERENCES


1. D. Grosenick, H. Wabnitz, H. Rinneberg, K.T. Moesta, and P. Schlag, Detection and characterization of breast tumors by a laser pulse mammography, *Biomedical Optical Meetings Technical Digest, Optical Society of America, Conference Edition*, pp. 380-382, 2000.

2. H. Rinneberg, D. Grosenick, K.T. Moesta, and P. Schlag, Detection and characterization of breast tumors by a laser pulse mammography, *Proc. Of Inter-Institute Workshop on In Vivo Optical Imaging at the NIH*, pp. 105-110, 1999.


# APPENDIX

None.